



HAL
open science

A variational framework for nonlinear viscoelastic models in finite deformation regime

E. Fancello, Jean-Philippe Ponthot, Laurent Stainier

► **To cite this version:**

E. Fancello, Jean-Philippe Ponthot, Laurent Stainier. A variational framework for nonlinear viscoelastic models in finite deformation regime. *Journal of Computational and Applied Mathematics*, 2008, 215 (2), pp.400-408. hal-01004968

HAL Id: hal-01004968

<https://hal.science/hal-01004968>

Submitted on 27 Aug 2019

HAL is a multi-disciplinary open access archive for the deposit and dissemination of scientific research documents, whether they are published or not. The documents may come from teaching and research institutions in France or abroad, or from public or private research centers.

L'archive ouverte pluridisciplinaire **HAL**, est destinée au dépôt et à la diffusion de documents scientifiques de niveau recherche, publiés ou non, émanant des établissements d'enseignement et de recherche français ou étrangers, des laboratoires publics ou privés.

A variational framework for nonlinear viscoelastic models in finite deformation regime

E.A. Fancello^a, J.P. Ponthot^b, L. Stainier^b

^a*Depto. de Engenharia Mecânica, Universidade Federal de Santa Catarina, Florianópolis, SC, Brazil*

^b*Aerospace and Mechanics Department (LTAS-MC&T), University of Liège, Belgium*

This work presents a general framework for constitutive viscoelastic models in the finite deformation regime. The approach is qualified as variational since the constitutive updates consist of a minimization problem within each load increment. The set of internal variables is strain-based and uses a multiplicative decomposition of strain in elastic and viscous components. Spectral decomposition is explored in order to accommodate, into analytically tractable expressions, a wide set of specific models. Moreover, it is shown that, through appropriate choices of the constitutive potentials, the proposed formulation is able to reproduce results obtained elsewhere in the literature. Finally, numerical examples are included to illustrate the characteristics of the present formulation.

MSC: 74C20; 74D10; 74S05; 35J50

Keywords: Finite viscoelasticity; Variational formulation; Constitutive updates

1. Introduction

In contrast with what we see in small strain regime, the choice of convenient internal variables and evolution laws for viscoelastic materials submitted to finite deformations is not trivial nor unique, leading to different formulations in the literature. We recall first the work of Simo [15] in which an additive decomposition of stresses in equilibrium and non equilibrium contributions is stated and the evolution law is defined as a linear differential equation on the non-equilibrium stresses. This approach was followed later by Holzapfel and Simo [5] and Holzapfel [3] or, more recently, [4,2]. Multiplicative decomposition of strains in viscous and elastic parts was applied by Sidoroff [14] and later to [9,7,8] among others. In [13] the ability of different models to reproduce nonlinear viscous behavior is discussed

and a model is proposed which is not restricted to small perturbations away from thermodynamic equilibrium. Another important reference that should be visited is [6].

The purpose of this work is to present a variational framework for constitutive viscoelastic models based on the formulation proposed in [11,12,17]. The constitutive updates satisfy a minimum principle within each load increment, feature that has the quality of providing appropriate mathematical structure for applications like error estimation among others (see [12]). The formulation assumes a multiplicative decomposition of strain into elastic and viscous components and a strain based set of internal variables, characteristic that relates it to the works [13] and the spatial model of [2] more than to the approach of Simo.

A particular difference between the present particularization and that used in plasticity or viscoplasticity [11] is related to the way in which inelastic strains are decomposed. While classic decomposition separates inelastic strains into *size* and *direction*, the present approach uses spectral decomposition that provides facilities to accommodate, into simple analytical expressions, a wide set of viscous models. It is also possible to show that an appropriate choice of constitutive potentials allows to reproduce other models in literature.

2. Variational form of constitutive equations

Using conventional notation, let us call $\mathbf{F} = \nabla_0 \mathbf{x}$ the gradient of deformations, and $\mathbf{C} = \mathbf{F}^T \mathbf{F}$ the Cauchy strain tensor, respectively. These values may be decomposed in volumetric and isochoric parts. The isochoric tensors are defined as follows:

$$\hat{\mathbf{F}} = \frac{1}{J^{1/3}} \mathbf{F}, \quad J = \det(\mathbf{F}), \quad \hat{\mathbf{C}} = \hat{\mathbf{F}}^T \hat{\mathbf{F}} = \frac{1}{J^{2/3}} \mathbf{F}^T \mathbf{F}. \quad (1)$$

We will work in the framework of irreversible thermodynamics, with internal variables. Thus, we define a general set $\mathcal{E} = \{\mathbf{F}, \mathbf{F}^i, \mathbf{Q}\}$ of external and internal variables, where \mathbf{F}^i is the inelastic part of the (total) deformation, and \mathbf{Q} contains all the remaining internal variables of the model. In addition, a multiplicative decomposition $\mathbf{F} = \mathbf{F}^e \mathbf{F}^i$ of the gradient of deformations is considered. We assume the existence of a free energy potential $W(\mathcal{E})$ and a dissipative potential $\phi(\dot{\mathbf{F}}; \mathcal{E})$, such that the Piola–Kirchhoff stress tensor, comprised of an equilibrium (elastic) and a dissipative (viscous) components, is derived as follows:

$$\mathbf{P} = \frac{\partial W}{\partial \mathbf{F}}(\mathcal{E}) + \frac{\partial \phi}{\partial \dot{\mathbf{F}}}(\dot{\mathbf{F}}; \mathcal{E}). \quad (2)$$

In addition, another dissipative potential $\psi(\dot{\mathbf{F}}^i, \dot{\mathbf{Q}}; \mathcal{E})$ is included to characterize the irreversible behavior related to the inelastic tensor \mathbf{F}^i , such that

$$\mathbf{T} = -\frac{\partial W}{\partial \mathbf{F}^i}(\mathcal{E}) = \frac{\partial \psi}{\partial \dot{\mathbf{F}}^i}(\dot{\mathbf{F}}^i, \dot{\mathbf{Q}}; \mathcal{E}), \quad \mathbf{A} = -\frac{\partial W}{\partial \mathbf{Q}}(\mathcal{E}) = \frac{\partial \psi}{\partial \dot{\mathbf{Q}}}(\dot{\mathbf{F}}^i, \dot{\mathbf{Q}}; \mathcal{E}). \quad (3)$$

It was shown in [11,17] that an incremental version of the above equations, constituting an incremental update method for the material state, can be obtained from the following incremental potential:

$$\mathcal{W}(\mathbf{F}_{n+1}; \mathcal{E}_n) = \Delta t \phi(\dot{\mathbf{F}}, \mathcal{E}_n) + \min_{\substack{\mathbf{F}_{n+1}^i \\ \mathbf{Q}_{n+1}}} \{W(\mathcal{E}_{n+1}) - W(\mathcal{E}_n) + \Delta t \psi(\dot{\mathbf{F}}^i, \dot{\mathbf{Q}}; \mathcal{E}_n)\}, \quad (4)$$

where $\dot{\mathbf{F}}(\mathbf{F}_{n+1}, \mathcal{E}_n)$, $\dot{\mathbf{F}}^i(\mathbf{F}_{n+1}^i, \mathcal{E}_n)$ and $\dot{\mathbf{Q}}(\mathbf{Q}_{n+1}, \mathcal{E}_n)$ are appropriate incremental approximations of $\dot{\mathbf{F}}$, $\dot{\mathbf{F}}^i$ and $\dot{\mathbf{Q}}$, respectively.

3. A set of viscoelastic models

A general set of isotropic³ viscoelastic materials based on the presented variational framework is proposed.

³ The isotropy condition is now assumed but no theoretical material symmetry constraints are inherent to the present formulation.

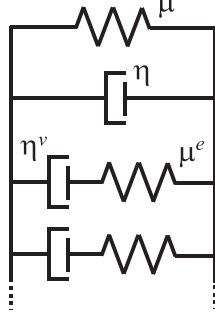


Fig. 1. Generalized Kelvin–Maxwell model.

To this aim, consider the classical rheological mechanism shown in Fig. 1 and the following assumptions:

- The elastic part of the Kelvin branch is split in isochoric and volumetric energies. The isochoric part is an isotropic function of $\hat{\mathbf{C}} = \hat{\mathbf{F}}^T \hat{\mathbf{F}}$:

$$\varphi(\hat{\mathbf{C}}) = \varphi(c_1, c_2, c_3), \quad (5)$$

where c_j are the eigenvalues of $\hat{\mathbf{C}}$. The volumetric part may be defined using the usual expression $U(J) = (K/2)[\ln J]^2$, The viscous part of the Kelvin branch is an isotropic function of the symmetric part of the rate of deformation:

$$\phi(\mathbf{D}) = \phi(d_1, d_2, d_3) \quad \text{with} \quad \mathbf{D} = \text{dev}(\text{sym}(\dot{\mathbf{F}}\mathbf{F}^{-1})), \quad (6)$$

where d_j are the eigenvalues of \mathbf{D} .

- The Maxwell branch is based on a multiplicative split of strains in an elastic and an isochoric viscous part

$$\hat{\mathbf{F}} = \hat{\mathbf{F}}^e \mathbf{F}^v \implies \hat{\mathbf{F}}^e = \hat{\mathbf{F}} \mathbf{F}^{v-1}, \quad \det \mathbf{F}^v = 1. \quad (7)$$

A flow rule for the internal variable \mathbf{F}^v can be written as

$$\dot{\mathbf{F}}^v = \mathbf{D}^v \mathbf{F}^v = (d_j^v \mathbf{M}_j^v) \mathbf{F}^v, \quad (8)$$

in which the spectral decomposition of $\mathbf{D}^v = \text{sym}(\dot{\mathbf{F}}^v \mathbf{F}^{v-1})$ in eigenvalues d_j^v and eigenprojections \mathbf{M}_j^v , $j=1, 2, 3$, was used. The scalars d_j are chosen to be the internal variables contained in the set $\hat{\mathbf{Q}} = \{d_1, d_2, d_3\}$. In this case, it is important to note that (8) is a constraint relating the internal variables \mathbf{F}^v and \mathbf{Q} . The elastic and viscous potentials associated to this branch are assumed to be isotropic functions of the elastic deformation and viscous stretching, and thus depend on their eigenvalues:

$$\varphi^e(\hat{\mathbf{C}}^e) = \varphi^e(c_1^e, c_2^e, c_3^e) \quad \text{and} \quad \psi(\mathbf{D}^v) = \psi(d_1^v, d_2^v, d_3^v), \quad (9)$$

where c_j^e are the eigenvalues of $\hat{\mathbf{C}}^e$.

- An incremental expression for the viscous deformation is obtained by using the classical exponential mapping [1,10] with the convenient property of providing an isochoric tensor for any traceless argument:

$$\Delta \hat{\mathbf{F}} = \hat{\mathbf{F}}_{n+1} \hat{\mathbf{F}}_n^{-1} = \exp[\Delta t \mathbf{D}] \implies \mathbf{D} = \frac{\Delta q_j}{\Delta t} \mathbf{M}_j = \frac{1}{2\Delta t} \ln(\Delta \hat{\mathbf{C}}). \quad (10)$$

$$\Delta \mathbf{F}^v = \mathbf{F}_{n+1}^v \mathbf{F}_n^{v-1} = \exp[\Delta t \mathbf{D}^v] \implies \mathbf{D}^v = \frac{\Delta q_j^v}{\Delta t} \mathbf{M}_j^v = \frac{1}{2\Delta t} \ln(\Delta \mathbf{C}^v). \quad (11)$$

Expressions (10) and (11) show that \mathbf{D} and \mathbf{D}^v are approximated by incremental expressions of $\Delta \hat{\mathbf{C}}$ and $\Delta \mathbf{C}^v$, respectively.

Taking into account (10) and (11), the minimizing variables $\mathbf{Q}_{n+1}, \mathbf{F}_{n+1}^v$ in (4) are replaced by the new incremental variables $\Delta q_j^v, \mathbf{M}_j^v$.

$$\begin{aligned} \mathcal{W}(\mathbf{F}_{n+1}; \mathcal{E}_n) = \mathcal{W}(\mathbf{C}_{n+1}; \mathcal{E}_n) = & \Delta\varphi(\hat{\mathbf{C}}_{n+1}) + \Delta t \phi \left(\frac{\Delta q_j^v}{\Delta t} \right) + \Delta U(\theta_{n+1}) \\ & + \min_{\mathbf{M}_j^v, \Delta q_j^v} \left\{ \Delta\varphi^e(\hat{\mathbf{C}}_{n+1}^e) + \Delta t \psi \left(\frac{\Delta q_j^v}{\Delta t} \right) \right\}, \end{aligned} \quad (12)$$

such that

$$\Delta q_j^v \in K_Q = \{p_j \in \mathbb{R} : p_1 + p_2 + p_3 = 0\}, \quad (13)$$

$$\mathbf{M}_j^v \in K_M = \{\mathbf{N}_j \in \text{Sym} : \mathbf{N}_j \cdot \mathbf{N}_j = 1, \mathbf{N}_i \cdot \mathbf{N}_j = 0, i \neq j\}, \quad (14)$$

where *Sym* is the set of symmetric second order tensors. The minimization operation is performed within the sets K_Q and \mathbf{D}^v , i.e. null trace of the viscous increment and orthogonality of eigenprojections, respectively. Given isotropic expressions for energy functions, the minimization in (12) can be performed in part analytically. A simple extension to this model can be obtained by considering a set of P Maxwell branches, as seen in Fig. 1(a).

4. Hencky and Ogden models

Hencky models are based on quadratic forms of logarithmic strain tensors:

$$\varphi = \mu \sum_{j=1}^3 (\varepsilon_j)^2, \quad \phi = \eta \sum_{j=1}^3 (d_j)^2, \quad (15)$$

$$\varphi^e = \mu^e \sum_{j=1}^3 (\varepsilon_j^e)^2, \quad \psi = \eta^v \sum_{j=1}^3 (d_j^v)^2. \quad (16)$$

In this case, it is particularly convenient to obtain simple uncoupled linear expressions for the minimizing argument Δq_j^v . In spite of the facility offered by Hencky models in terms of analytical treatment, it is well known that this type of hyperelastic potentials does not fit well the behavior of rubber-like materials. For that case, a more adequate choice may be the Ogden model which has also the capability of generalizing other models like neo-Hookean and Mooney–Rivlin. Ogden models are based on the following potentials:

$$\varphi = \sum_{j=1}^3 \sum_{p=1}^N \frac{\mu_p}{\alpha_p} ([\exp(\varepsilon_j)]^{\alpha_p} - 1), \quad \phi = \sum_{j=1}^3 \sum_{p=1}^N \frac{\eta_p}{\alpha_p} ([\exp(d_j)]^{\alpha_p} - 1), \quad (17)$$

$$\varphi^e = \sum_{j=1}^3 \sum_{p=1}^N \frac{\mu_p^e}{\alpha_p} ([\exp(\varepsilon_j^e)]^{\alpha_p} - 1), \quad \psi = \sum_{j=1}^3 \sum_{p=1}^N \frac{\eta_p^v}{\alpha_p} ([\exp(d_j^v)]^{\alpha_p} - 1). \quad (18)$$

5. Numerical implementation and examples

Since the present constitutive equations allow nearly incompressible behaviors, appropriate finite element spaces are necessary to circumvent the volumetric locking. Therefore, the equilibrium problem was expressed using the variational formulation proposed in [16] in which the pressure field π and volumetric strain field θ are assumed to be constant over each element. The examples shown in this paper are run with isoparametrical eight nodes brick elements.

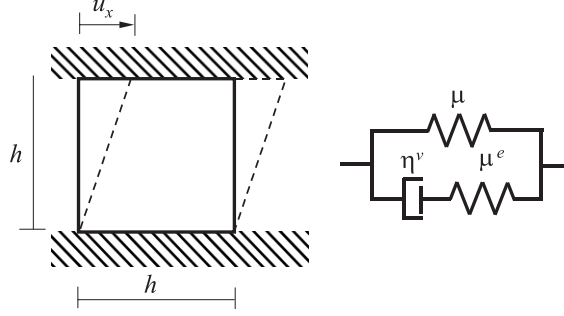


Fig. 2. Cyclic shear test.

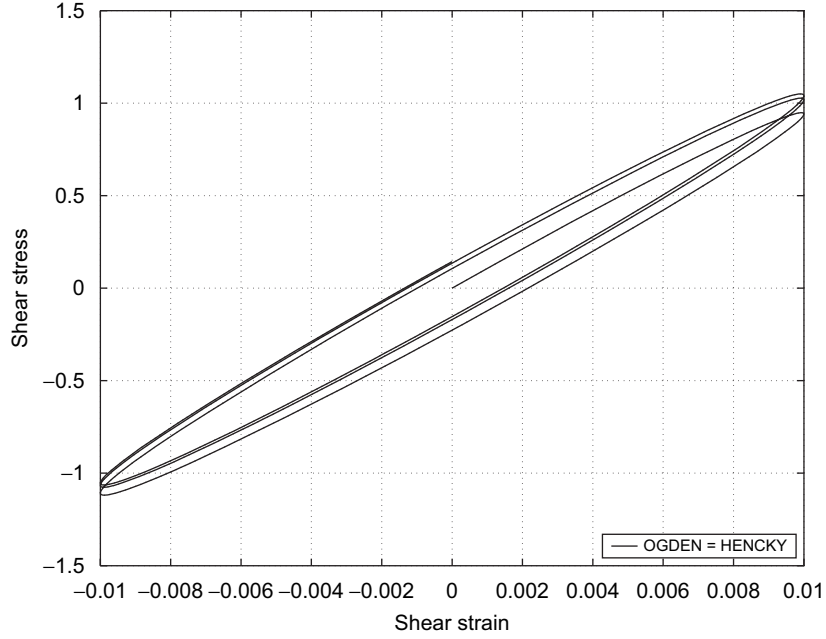


Fig. 3. Stress–strain curves in cyclic shear test. Amplitude: 0.01.

5.1. Shear test

In this example a single 3D element is submitted to a pure shear deformation (Fig. 2). The material behavior follows the rheological model of Fig. 1(b) with identical material parameters used in an equivalent example presented in [13]. The lateral displacement u_x follows a sinusoidal law $u_x = U \sin wt$, where $w = 0.3 \text{ s}^{-1}$.

The material is quasi incompressible due to a penalizing bulk modulus K . Two different models for φ were used: Ogden model and Hencky model. In the case of Ogden, we used the following six-parameter fitting: $\mu_1 = 20$, $\mu_2 = -7$, $\mu_3 = 1.5$, $\alpha_1 = 1.8$, $\alpha_2 = -2$, $\alpha_3 = 7$.

For the Hencky model, the value $\mu = \sum_i \frac{1}{2} \mu_i \alpha_i = 30.25$ was used, which is the consistent equivalent shear modulus for small deformations. The Maxwell branch uses Hencky model for both potentials with $\mu^e = 77.77$ and viscous coefficient η^v such that $\tau = \eta^v / \mu^e = 17.5$.

The time evolution of Cauchy stresses σ_{xy} as a function of shear strain C_{xy} , for different shear amplitudes, is shown in Figs. 3–5. In the case of small strains both models (Ogden or Hencky main spring) give identical results, and match quite well equivalent results in [13]. As expected, the behavior of the main spring is determinant on the behavior of the whole system for deformations higher than unity.

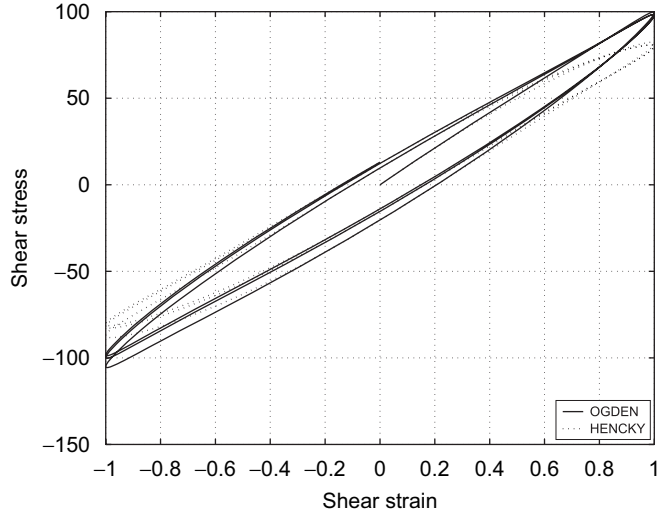


Fig. 4. Stress–strain curves in cyclic shear test. Amplitude: 1.0.

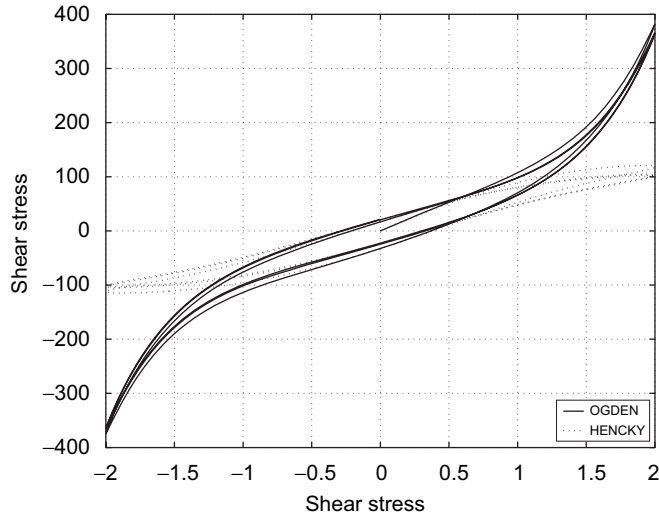


Fig. 5. Stress–strain curves in cyclic shear test. Amplitude: 2.0.

Comparing the results of the Ogden-based model with those of [13] it is possible to see a close correlation of maximum values of stress for all four cases. However, hysteresis loops clearly look “thinner” as the deformation grows along the cycle. This behavior is in agreement with the fact that the Hencky model used in the Maxwell branch provides a contribution in stress significantly lower than a corresponding Ogden model for high deformations.

6. Pinched thick plate

This example shows a thick viscoelastic plate with clamped boundary and in contact with a rigid hemispherical tool performing the path given in Fig. 6. The tool initially presses the plate down to a cursor-end position where it remains during a relaxing period. Finally, it is removed at high velocity. According to the initial tool velocity defined by the time t different deformation histories are obtained. Three cases are tested with $t = 0.5, 1,$ and 2 s. This run was performed taking advantage of symmetry conditions and a mesh of $16 \times 16 \times 5$ brick elements.

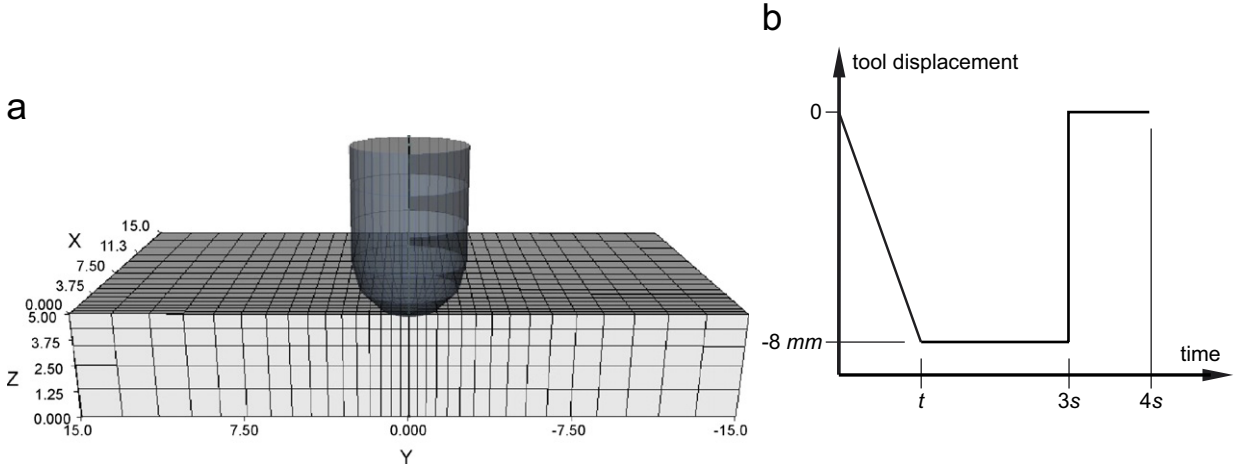


Fig. 6. (a) Pinched plate. (b) Tool path.

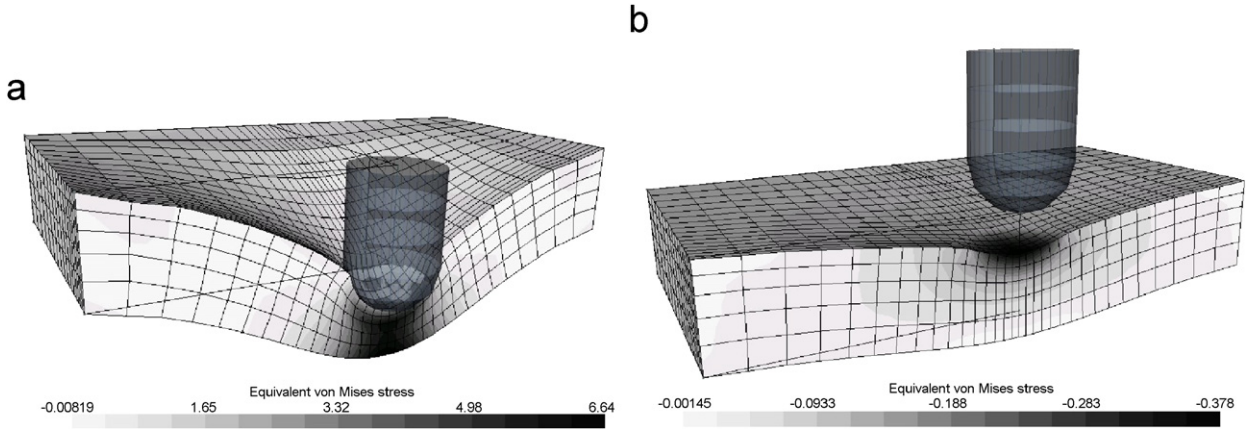


Fig. 7. Pinched plate. (a) Intermediate and (b) final configurations.

The square plate is 30 mm wide and 5 mm high. The tool has a radius of 2.5 mm and its displacement is 8 mm. Both elastic potentials φ and φ^e use an Ogden model with the following material parameters: $\mu_1 = 2.758$; $\mu_2 = -1.725$; $\mu_3 = 0.704$ (MPa) and $\alpha_1 = 1.33$; $\alpha_2 = -3.05$; $\alpha_3 = 3.89$. The viscous potential ψ is of Hencky type with $\eta^v = 1.1394$ ($\tau = 2$ s). Potential ϕ is null.

Fig. 7(a) shows the deformed configuration for the maximum tool displacement, while 7(b) illustrates the final configuration after the tool removal. Figs. 8 and 9 present the history of the Cauchy stress σ_x and vertical displacement of the point located on the plate bottom surface just below the punch tip. These curves show clearly that faster tool motions produce higher stresses and higher dissipated energy with a consequent faster tool-piece separation during the backward motion.

7. Final remarks

A general set of viscoelastic constitutive models is presented in this article. Due to its variational characteristic it provides appropriate mathematical structure for further applications like, for example, error estimation. Moreover, it has the appealing characteristic that different materials can be modelled by means of the definition of constitutive potentials depending on eigenvalues of strains and strain-rates. As a practical consequence, most of the implementation effort, including stress updates and tangent matrix is done at generic level with no relation to a specific isotropic law

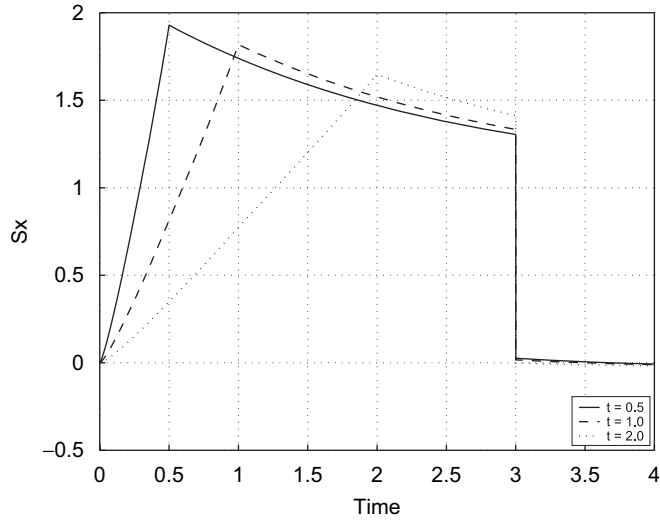


Fig. 8. Cauchy stress σ_x versus time.

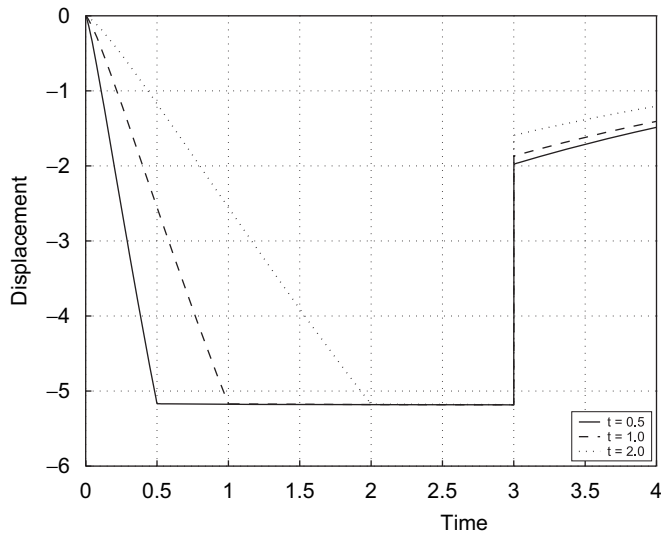


Fig. 9. Displacement u_z of lower surface below punch tip.

(potential). Moreover, the three-equation nonlinear system that provide the stress and strain updates is analytically invertible and the material tensor has a closed form expression. Thus, the performance of the constitutive update is comparable to that of the classical radial-return algorithm in elasto-plastic problem.

The first numerical example compares the capacity of Hencky and Ogden-type models to reproduce observed nonlinear viscous behavior. As expected, Ogden models perform better for the case of large strains and rubber-like materials, leading to non-elliptic hysteretic loops. The second example illustrate the application of the present model to common large scale FEM computations.

References

- [1] L. Anand, G. Weber, Finite deformations constitutive equations and a time integration procedure for isotropic hyperelastic-viscoplastic solids, *Comput. Methods Appl. Mech. Eng.* 79 (1990) 173–202.
- [2] J. Bonet, Large viscoelastic constitutive models, *Internat. J. Solids Struct.* 38 (2001) 2953–2968.

- [3] G.A. Holzapfel, On large viscoelasticity: continuum formulation and finite element applications to elastomeric structures, *Internat. J. Numer. Methods Eng.* 39 (1996) 3903–3926.
- [4] G.A. Holzapfel, T.C. Gasser, A viscoelastic model for fiber-reinforced composites at finite strains: continuum basis, computational aspects and applications, *Comput. Methods Appl. Mech. Eng.* 190 (2001) 4379–4403.
- [5] G.A. Holzapfel, J. Simo, A new viscoelastic constitutive model for continuous media at finite thermomechanical changes, *Internat. J. Solids Struct.* 33 (1996) 3019–3034.
- [6] P. Le Tallec, *Numerical Analysis of Viscoelastic Problems*, vol. 109, Masson, Paris, France, 1993, pp. 223–258.
- [7] P. Le Tallec, C. Rahier, A. Kaiss, Three-dimensional incompressible viscoelasticity in large strains: formulation and numerical approximation, *Comput. Methods Appl. Mech. Eng.* 109 (1993) 223–258.
- [8] A. Lion, A constitutive model for carbon filled rubber, experimental investigation and mathematical representations, *Continuum Mech. Thermodyn.* 8 (1996) 153–169.
- [9] J. Lubliner, A model of rubber viscoelasticity, *Mech. Res. Commun.* 12 (1985) 93–99.
- [10] C. Miehe, Exponential map algorithm for stress updates in anisotropic multiplicative elastoplasticity for single crystals, *Internat. J. Numer. Methods Eng.* 39 (1996) 3367–3390.
- [11] M. Ortiz, L. Stainier, The variational formulation of viscoplastic constitutive updates, *Comput. Meth. Appl. Mech. Eng.* 171 (1999) 419–444.
- [12] R. Radovitzky, M. Ortiz, Error estimation and adaptive meshing in strongly nonlinear dynamic problems, *Comput. Methods Appl. Mech. Eng.* 172 (1999) 203–240.
- [13] S. Reese, S. Govindjee, A theory for finite viscoelasticity and numerical aspects, *Internat. J. Solids Struct.* 35 (1998) 3455–3482.
- [14] F. Sidoroff, Un modèle viscoélastique non linéaire ave configuration intermédiaire, *J. Mécanique* 13 (1974) 679–713.
- [15] J.C. Simo, On a fully three dimensional finite-strain viscoelastic damage model: formulation and computational aspects, *Comput. Methods Appl. Mech. Eng.* 60 (1987) 153–173.
- [16] J.C. Simo, R.L. Taylor, Quasi incompressible finite elasticity in principal stretches, Continuum basis and numerical algorithms, *Comput. Methods Appl. Mech. Eng.* 85 (1991) 273–310.
- [17] L. Stainier, Une formulation variationnelle des algorithmes de calcul des contraintes pour les modèles élastoviscoplastiques et viscoélastiques en grandes transformations, in: 6ème Colloque National en Calcul des Structures, Giens, France, 2003.